

Neutrophil Chemotaxis in Moving Gradients

Mohammad A. Qasaimeh,* Michal Pyzik, Mélina Astolfi, Silvia M. Vidal,
and David Juncker*

Neutrophils are known to rapidly migrate to sites of infection and injury, and track bacteria guided by spatiotemporally controlled chemokine gradients. Previous studies of neutrophil chemotaxis, using micropipettes and lately microfluidic devices, are limited to stationary sources and gradients. Thus, despite the well-known ability of neutrophils to track bacteria *in vitro*, their response to defined moving gradients remains unknown. Here, a “floating” concentration gradient of interleukin-8 is generated using a microfluidic quadrupole, and neutrophils cultured in a Petri dish are challenged with steep stationary and moving gradients. Individual neutrophils are tracked by live microscopy and their chemotaxis is analyzed. Interestingly, neutrophils are shown to enter the gradient region in a rolling-like behavior, rapidly adhere to the bare dish, and polarize within 30 s, faster than what has been observed to date. Under stationary gradients, neutrophil migration length is maximal for cells located at the low end of the gradient, whereas under moving gradients, neutrophils migrate over longer distances and the length travelled is independent of their starting position. Furthermore, neutrophils are shown to initiate their migration at a maximum speed, slowing down when migrating deeper into the gradient and eventually stopping. This work lays the foundation for future chemotaxis assays with moving gradients.

processes such as wound healing and inflammation.^[1] They are highly dynamic and migrate rapidly in response to gradients of chemokines, a process known as chemotaxis.^[2] Chemotactic factors can be from a pathogen-derived source such as *N*-formyl-methionyl-leucyl-phenylalanine (fMLP) or host-produced cytokines such as interleukin-8 (IL-8) and leukotriene B₄ (LTB₄).^[2] Neutrophil chemotaxis has been studied over the last 50 years using a range of gradient generation techniques^[3,4] that have shaped our current understanding of neutrophil activation, polarization,^[5] signaling mechanisms and pathways,^[6] neutrophil recruitment,^[7] and reverse migration,^[8] as well as neutrophil dysfunctions that are associated with diseases.^[9] Nonetheless, current methods available for the study of chemotaxis are limited. The micropipette assay, a classical method dating back to the 1970s, is often used to rapidly apply local pulses of diffusible cues^[4,10] and helped to illustrate the capability of neutrophil reorientation in changing gradients.^[11]

1. Introduction


Neutrophils represent an important component of the first defense barrier against infections, and play a key role in several

Although the micropipette assays are quick, they lack reproducibility and precise gradient control. Microfluidic gradients offer spatiotemporal control and can be maintained over several hours.^[12] Multiple microfluidic chips have been developed

Prof. M. A. Qasaimeh, M. Astolfi, Prof. D. Juncker
Biomedical Engineering Department
McGill University
Montréal, QC H3A 0G1, Canada
E-mail: mohammad.qasaimeh@nyu.edu; david.juncker@mcgill.ca

Prof. M. A. Qasaimeh
Division of Engineering
New York University Abu Dhabi
Abu Dhabi 129188, UAE

Prof. M. A. Qasaimeh
Department of Mechanical and Aerospace Engineering
New York University
NY 11201, USA

 The ORCID identification number(s) for the author(s) of this article can be found under <https://doi.org/10.1002/adbi.201700243>.

© 2018 The Authors. Published by WILEY-VCH Verlag GmbH & Co. KGaA, Weinheim. This is an open access article under the terms of the Creative Commons Attribution-NonCommercial License, which permits use, distribution and reproduction in any medium, provided the original work is properly cited and is not used for commercial purposes.

DOI: 10.1002/adbi.201700243

Dr. M. Pyzik, Prof. S. M. Vidal
Department of Human Genetics
McGill University
Montréal, QC H3G 0B1, Canada

Dr. M. Pyzik
Division of Gastroenterology
Department of Medicine
Brigham & Women's Hospital
Harvard Medical School
Boston, MA 02115, USA

Prof. D. Juncker
Genome Quebec Innovation Centre
McGill University
Montréal, QC H3A 0G1, Canada

Prof. D. Juncker
Department of Neurology and Neurosurgery
McGill University
Montréal, QC H3A 1A4, Canada

over the last decade to study neutrophil chemotaxis under stationary,^[13] temporally evolving,^[14] reversing,^[8,15] and opposing gradients,^[16] and have been used for the study of neutrophil chemotactic memory,^[17] polarization,^[5] rolling,^[18] trafficking^[7] and swarming,^[19] interaction with endothelial cells,^[20] and their antimicrobial repertoire role,^[21] to name a few.

Conventional microfluidic gradient generators are formed within closed microchannels, which require adherent cells to be introduced and cultured in the microchannel before gradients are applied, and limit the ability to move the gradient afterward. Neutrophils *in vivo* are “flowed” into the gradient, resulting in their activation and migration to the site of infection, and subject to fluctuating and moving chemotactic environments such as when chasing bacteria at wound sites.^[22] The classic 1959 video by David Rogers documents the neutrophil’s response to a moving source of chemokines showing it chasing bacteria (*Staphylococcus aureus* microorganisms) in solution. Yet after all these years, many open questions remain with respect to the response of neutrophils to a chemokine moving source and gradient. For example, it is still unknown how neutrophil’s response changes over time during chemotaxis, how quickly they get desensitized within gradients, what is the influence of the chemotactic memory effect,^[17] how dynamic chemotactic environments contribute to their trafficking,^[7] and how their migration is affected by a moving gradient. Hence, experimental studies to characterize neutrophil chemotaxis under moving gradients are needed.

A closed-channel microfluidic device was proposed for studying gradient-induced neutrophil desensitization,^[23] and as a proof of concept, the authors were able to hydrodynamically move the gradient for 25 μm only. More recently, a noteworthy microfluidic system was developed to maintain migrating neutrophils in the same place within an LTB_4 concentration gradient.^[24] The system changed the position of the neutrophil within the gradient in synchronicity with its chemotaxis using a feedback control, and thus eliminated the temporal concentration effect. However, to provide physiologically relevant conditions of moving gradients, neutrophils should encounter both temporal and spatial concentration gradient effects, where their interplay controls the cell response. We previously introduced the microfluidic quadrupole (MQ) and the generation of floating concentration gradients.^[25] The hallmarks of these floating gradients are that they can be rapidly adjusted by tuning the flow rates; they feature shear stress-free zones; and they can be moved across a flat surface by either displacing the substrate or the microfluidic probe (MFP)^[26] used to form them. An important benefit of using an MFP is that cell culture can be performed in conventional Petri dishes, which are then mounted on a microscope, followed by the application of the gradient to the selected cells.

Here, we use the MQ and apply floating concentration gradients of IL-8 on fresh human neutrophils, obtained from peripheral blood of healthy volunteers and cultured in Petri dishes (Figure 1). We discuss our findings in rapid neutrophil activation and reveal their interaction (i.e., rolling-like and arrest behavior) with substrates upon entering the gradient region. Further, we apply stationary and moving IL-8 gradients to neutrophils and compare their response time, migration distance, and speed at the single cell level.

2. Results

2.1. IL-8 Concentration Gradient Atop a Culture of Neutrophils

Before starting the experiment, the MFP was lowered to an empty Petri dish and the MFP tip was aligned parallel to the dish. Then, the neutrophil-containing Petri dish was positioned on the microscope stage under the MFP, as shown in Figure 1a,b. The experiment starts with simultaneous injection and aspiration through the fluidic apertures, generating a floating concentration gradient on the top of neutrophils (Figure 1c,d). The experimental setup is further detailed in the “Experimental Section.”

The gradient stability was analyzed by examining the gradient width and fluorescent relative intensity with respect to time (see Figure 1e). The gradient reached steady state within a few tens of seconds after the fluid flow was initiated. The gradient width varied between 74 and 76 μm , in excellent agreement with 3D numerical simulations that yielded a 75 μm gradient width (see Figure S1 in the Supporting Information). Variations in the gradient width are caused by small and rapid movements of the gradient around its center position, produced by bubbles in the syringes and glass capillaries, or mechanical vibrations that may affect the gap between the MFP and the Petri dish. The jump in gradient width at ≈ 700 s is ascribed to a bubble, but remained a rare occurrence.

2.2. Rapid Neutrophil Activation, Rolling, and Adhesion within IL-8 Gradient

Neutrophils were isolated from the blood of healthy donors with a purity of $>97\%$ (Figure S2, Supporting Information). At the time of the experiment, neutrophils were found either adherent to the bottom of the dish or free-floating in the culture medium. Adherent neutrophils were unaffected by the fluid flow, but suspended neutrophils were continuously being drawn into the gap below the MFP, and some of them into the aspiration apertures.

The generated gradient can be moved with respect to adherent neutrophils; therefore, we were able to expose neutrophils to stationary gradients at the time of our choice. We exposed neutrophils to stationary IL-8 gradient at $t = 0$ s by moving the microscope stage with respect to the gradient, and then measured the time required for neutrophils to respond. In these experiments, we analyzed all cells within the field of view.

Neutrophils quickly responded to the gradient by changing their shape and becoming polarized, and then migrating toward the higher concentration of IL-8 (Video S1 in the Supporting Information). As illustrated with a representative example in Figure 2a, a single neutrophil underwent polarization in less than 30 s upon exposure to the gradient. Polarization is defined as an apparent change in the circular cell shape with extending leading edge more than 25% of cell original diameter, and the polarization time is measured from the “round” state of neutrophils. These results set a new lower limit on the activation time of neutrophils that had previously been reported as 90 s^[27] and 2 min.^[28] Further analysis from three separate experiments revealed that all polarized cells ($n = 36$) initiated migration in less than 120 s

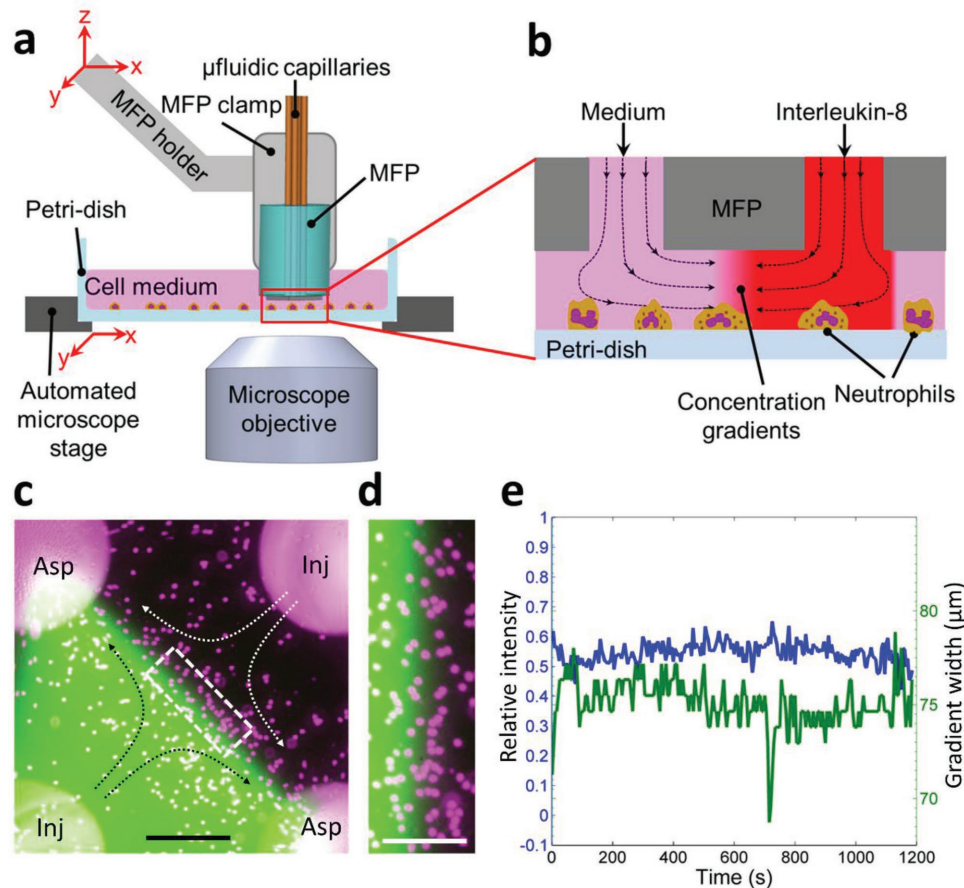


Figure 1. Floating concentration gradients of IL-8 for the study of neutrophil chemotaxis. a) Schematics of the experimental setup including the microfluidic probe (MFP) and a Petri dish seeded with fresh neutrophils. The floating gradients are established within the microfluidic quadrupole (MQ) in the gap between the MFP and the dish. b) An enlarged view showing neutrophils exposed to 100% IL-8 (red, positive control), to 0% IL-8 (negative control), and within the IL-8 concentration gradient. c) Fluorescent microscopic image showing the distribution of IL-8 which covers the bottom left of the image, and is absent in the top right while in between forming the concentration gradient. Injection and aspiration apertures are labeled as “Inj” and “Asp,” respectively. FITC-Dextran (green) was mixed to the IL-8 solution for visualization and the neutrophils were labeled with eFluor670-proliferation dye (magenta). Dashed curved arrows indicate flow direction. Scale bar is 200 μm . d) Close-up view of neutrophils enclosed within the white dashed box shown in panel (c). Scale bar is 100 μm . e) Time course of position (blue curve) and width (green curve) of the IL-8 concentration gradients in the center of the MQ (stagnation point). Position is measured as the location of the point with 0.5 relative fluorescence intensity, and width is measured as the distance between 0.1 and 0.9 of the relative fluorescence intensity.

(85 \pm 16 s), where migration initiation is defined as cell traveling by at least half of its original diameter (from center to center).

While suspended neutrophils were carried by the fluid flow, we observed some of them attaching to the surface of the plate once entering the concentration gradient zone, a phenomenon similar to the one previously shown for neutrophil capture on substrates coated with E-Selectin.^[29] However, neutrophils here were attaching to a pristine plate which was repeatedly observed as the gradient was moved to new, previously unexposed areas, suggesting a rapid adhesion mechanism with the glass. Figure 2b shows neutrophils being drawn in with the flow at $t = 0$ s, and five neutrophils attached to the substrate in the gradient area at $t = 240$ s. Upon moving the MFP and the gradient to the left with respect to the dish ($t = 960$ s), we observed three new neutrophils attached to the substrate. When moving the gradient to a new position, neutrophils attached to the substrate under the gradient, with no neutrophils attaching to regions that were previously exposed to the gradient. More details of

neutrophil capture at various positions within the gradient are shown in Video S2 in the Supporting Information. Neutrophil attachment in the gradient region only implies that attachment is the result of neutrophil activation after entering the IL-8 concentration gradient, which raises the possibility of an IL-8 receptor–dependent mechanism for rapid neutrophil adhesion.

Captured neutrophils were observed to polarize and start migrating toward the higher concentration of IL-8. We tracked individual neutrophils and observed activation within 35 \pm 8 s ($n = 8$), consistent with the 30 s measured previously (Figure 2a; see also the Video S2 in the Supporting Information). Exposure of neutrophils to IL-8 is known to activate integrin receptors and their conformational change on the cell surface,^[30] and studies have confirmed the importance of IL-8 for in vivo neutrophil arrest.^[31] Furthermore, rapid arrest (<1 s) of neutrophils^[32] and monocytes^[33] on cultured endothelial cells was observed after treatments with IL-8. Moreover, neutrophils rolling on a substrate coated

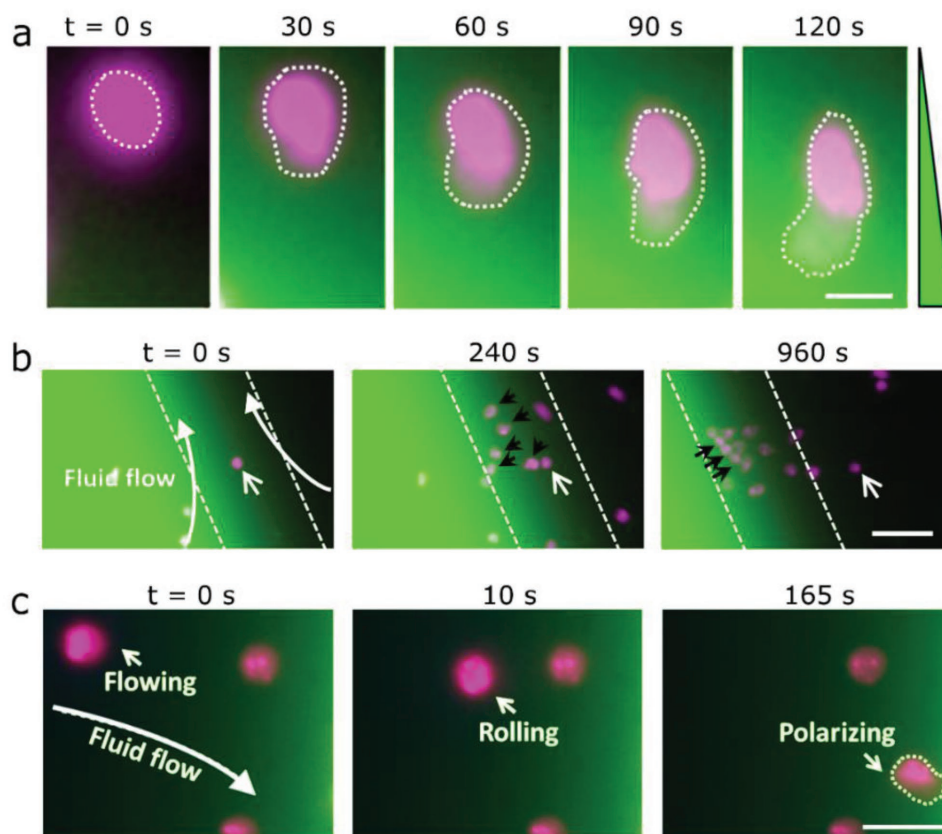


Figure 2. Neutrophil response to floating IL-8 gradients. a) Time-lapse microscopic images of a single neutrophil polarization. Scale bar is 10 μm . b) Neutrophils rapidly adhering to the substrate within the gradient region. The gradient width is enclosed by the white dashed lines, captured neutrophils denoted by black arrows, one reference “immobile” neutrophil is denoted by a white arrow across the frames, and the flow is shown by the curved arrow (see Video S2 in the Supporting Information for more details). Scale bar is 50 μm . c) Neutrophil rolling-like motion and adhesion, followed by polarization and migration toward the higher concentration of the gradient (see Video S3 in the Supporting Information for more details). Scale bar is 25 μm .

with adhesion molecules were shown to arrest after exposure to IL-8 in solution.^[34] Nonetheless, this study is the first to observe neutrophil arrest on uncoated substrates within a soluble IL-8 gradient. Further studies using the developed setup could allow for better understanding of the underlying intracellular mechanism of neutrophil arrest and polarization within concentration gradients.

High magnification (40 \times) time-lapse imaging revealed neutrophil rolling-like behavior followed by adhesion to the substrate, seemingly replicating the rolling of neutrophils on the inner wall of blood vessels^[35] (Figure 2c; Video S3, Supporting Information). Cell rolling behavior is influenced by the fluid flow drag and the cell–substrate adhesive forces. Therefore, in the example shown in Figure 2c, cell rolling occurred on a curved path (from top left to bottom right) as a result of the bent path of fluid flow within the observation window. However, cell migration within the gradient, after sticking and polarization, occurred toward the higher concentration of the gradient that is almost perpendicular to the fluid flow path at that point. For better understanding of the fluid flow direction, see the dashed curved arrows in Figure 1c and the 3D flow streamlines in Figure S1 in the Supporting Information.

Neutrophil rolling velocity was measured around 4 $\mu\text{m s}^{-1}$ in the buffer area, slowing down following gradient zone entry, and

leading to immobilization in <5 s. Polarization occurred within 35 s, followed by migration toward higher IL-8 concentrations. Further analysis of additional rolling cells confirmed our measurements with a speed of $4 \pm 0.8 \mu\text{m s}^{-1}$ before being captured on the substrate ($n = 8$). The measured rolling speed of neutrophils matched reasonably with previous *in vivo* experiments measuring neutrophil rolling at an average speed of 3.8 $\mu\text{m s}^{-1}$.^[36] Fluid velocity in the observation window, measured from streaklines, was found to be about 26 $\mu\text{m s}^{-1}$, consistent with the simulation results (0–35 $\mu\text{m s}^{-1}$), suggesting that captured neutrophils were entering the gradient region with a rolling-like behavior rather than being suspended and carried by the fluid flow. Nevertheless, more experiments are required to confirm these observations and to understand the associated mechanisms.

2.3. Neutrophil Chemotaxis in Stationary IL-8 Concentration Gradients

Depending on the position of adhered neutrophils relative to the gradient, they were classified into one of five groups: negative control (NC) for neutrophils in the areas without IL-8, positive control (PC) for the ones exposed to 100% IL-8, and the gradient region that is categorized into 3 groups depending on

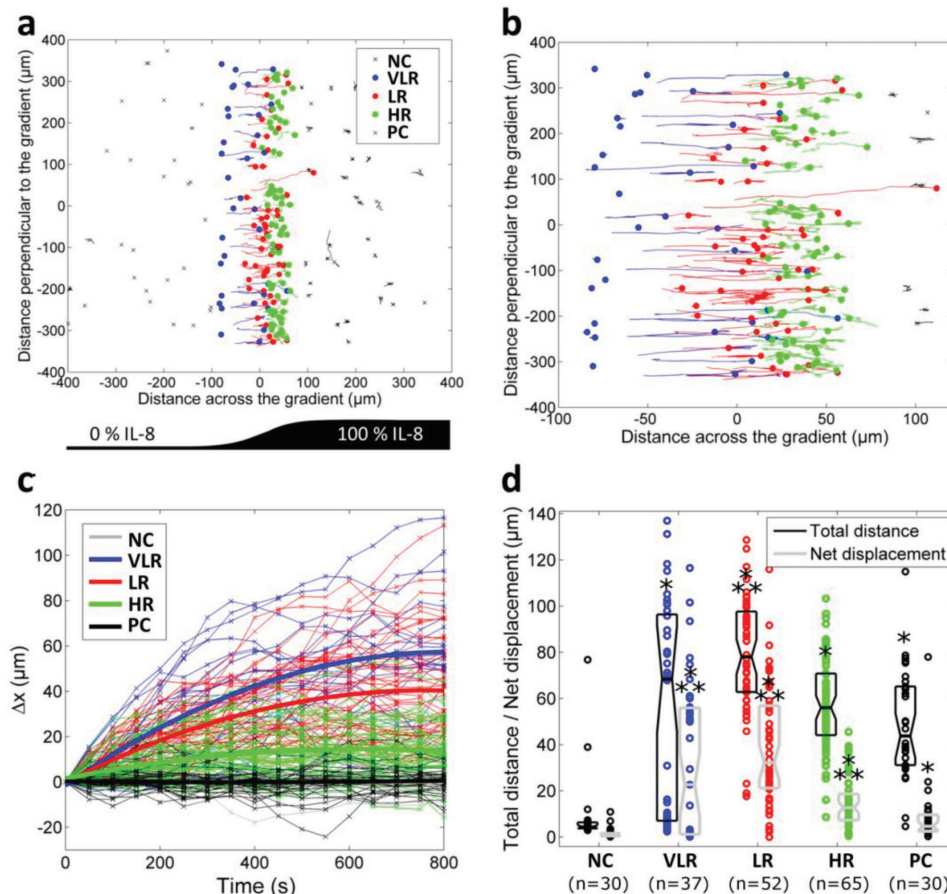


Figure 3. Neutrophil migration under stationary IL-8 concentration gradients. a) Tracks of neutrophil migration are colored based on their initial position group, while the dot indicates the end position. Negative control (NC) represents cells in areas without IL-8, positive control (PC) represents cells exposed to 100% IL-8, very low region (VLR) group denotes cells exposed to gradients below the 10% range, low region (LR) groups denote cells located in between 10% and 50% of the gradient, and high region (HR) groups denote cells between 50% and 90% of the gradient. b) An enlarged view of neutrophil tracks in the stationary gradient. c) Migration distance (Δx) of total 214 individual neutrophils (thin lines) and second-order polynomial fit of the average displacement (thick lines) for each group of neutrophils as a function of time for all tracks shown in panel (b). d) Dot plots and floating bars of the total distance and net displacement, respectively, for each group. Each open circle represents an individual neutrophil, and n is the total number of neutrophils in each group, analyzed from three separate experiments. Boxplots show the median, and the first and third quartiles for each group. Single star (*) indicates p -value < 0.05 when compared to NC, and double stars (**) indicates p -value < 0.05 when compared to PC (t -test).

neutrophils' initial position within the gradient. The gradient groups are: very low region (VLR), low region (LR), and high region (HR), see Figure S3 in the Supporting Information for more information. Tracks of individual neutrophils extracted from the time-lapse images (Video S4 in the Supporting Information) are shown in Figure 3a,b. Neutrophils exposed to the gradient migrated toward the higher concentration during the 800 s experiment. As expected, neutrophils in the PC group were activated and migrating randomly, while neutrophils from the NC group (not exposed to IL-8) showed little or no migration.

For individual cells, we analyzed the total travelled distance (d), which is defined as the length of the migration path over the course of the experiment, and the net displacement (Δx), which is defined as the migration distance in the direction of the gradient. Figure 3c depicts Δx with respect to time. Neutrophils from the control groups showed no significant net displacement, with observed oscillation around $\Delta x = 0$ during the experiment. Neutrophils from VLR and LR showed the greatest

Δx , with a few neutrophils migrating in excess of the gradient width (75 μm). Neutrophils from HR exhibited shorter Δx , and interestingly, they stopped before reaching the maximum value of the concentration. The average curve plateaus earlier for HR, indicating that cells in this group stopped moving earlier as they were closer to the 100% IL-8 region (for more details, see Figure S4 in the Supporting Information). Statistical analysis confirmed that Δx of neutrophils was correlated ($R^2 = 0.43$) to their initial position within the gradient, as shown in Figure 3d and Figure S5 in the Supporting Information.

Neutrophils with the VLR group were shown in two distinct subpopulations: migrating cells and "nearly" static cells (Figure 3d). LR showed the highest proportion of moving cells. Collectively, all gradient groups showed a significant increase in the Δx compared to both NC and PC. Likewise, gradient groups showed significant higher total travel distance " d " in comparison to nonexposed neutrophils (NC), but only LR neutrophils showed a significant increase in " d " when compared to PC.

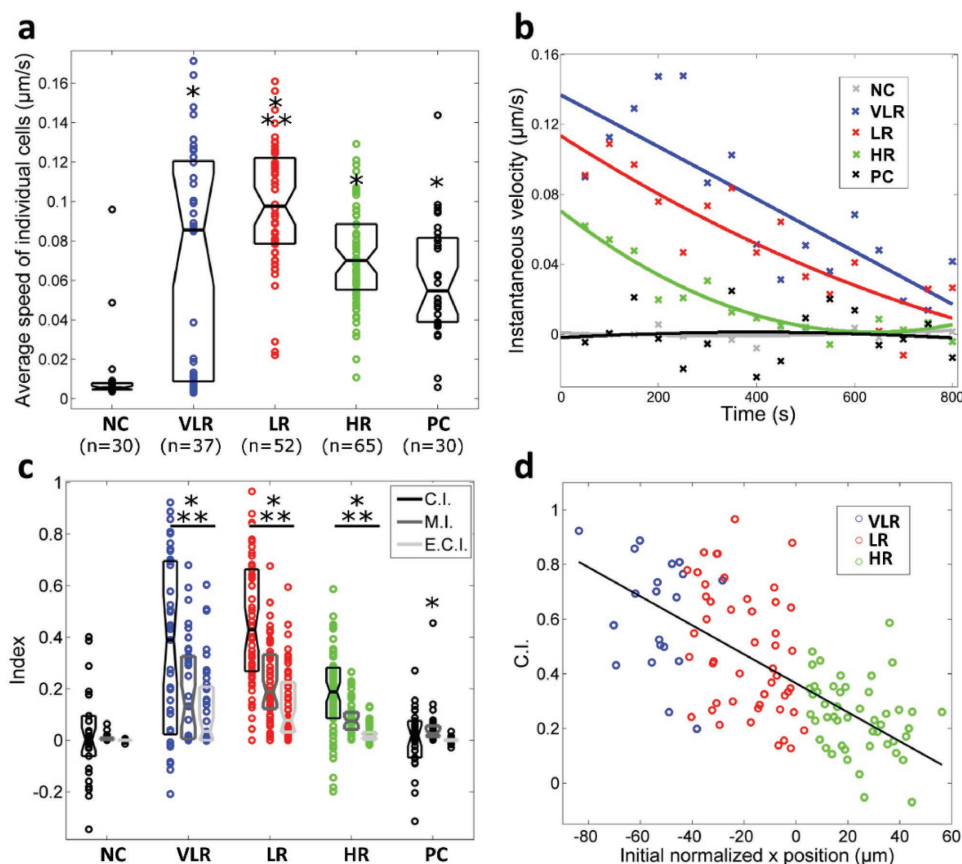


Figure 4. Migration and motility analysis of neutrophils under stationary IL-8 concentration gradients. a) Average cell migration speed for each group. n is the total number of neutrophils in each group, analyzed from three separate experiments. b) Average instantaneous migration velocity in gradient direction for each cell group. c) The chemotactic index (C.I.), motility index (M.I.), and effective chemotactic index (E.C.I.) for each group. C.I. denotes cell capability to move toward the gradient direction, M.I. signifies cell competence to move randomly, and E.C.I. represents cell capacity to move in both random and directional ways (E.C.I. = C.I. \times M.I.). d) The C.I. as a function of initial cell position along the gradient, where correlation coefficient $R^2 = 0.46$. Each open circle “o” represents an individual neutrophil and the cross “x” represents the group averaged value for each 50 s period while lines are fitted averages. n is the total number of neutrophils in each group. Boxplots show the median, and the first and third quartiles for each group. Single star (*) indicates p -value < 0.05 when compared to NC, and double stars (***) indicates p -value < 0.05 when compared to PC (t -test).

The average migration speed of neutrophils varied widely, with $5.4 \mu\text{m min}^{-1}$ on average within the gradient groups, significantly higher than those in the negative control region (Figure 4a). The speed of LR neutrophil migration was shown to be significantly higher than the speed within the positive control group. A time-course analysis of the instantaneous velocity reveals that migration speed is highest at the beginning of neutrophil activation, and continuously decreases with cells moving to higher IL-8 concentration; consistent with these findings, HR cells have the lowest velocity (Figure 4b). This is probably related to the quick saturation of the receptors and desensitization of the response to IL-8, as shown by the slopes in Figure 3c. These results are also reflected by our previous finding that most neutrophils stopped migrating when they reached the higher end of the gradient, with very few neutrophils traveling beyond. Neutrophil sensing mechanisms were responsive and quick to detect the plateau in the concentration of IL-8 after crossing the 90% of highest concentration of the gradient (22.5 ng mL^{-1} IL-8), suggesting that neutrophil receptors became saturated or desensitized before reaching the positive control region (100% IL-8 concentration). This can be confirmed in the future by applying gradients of

lower IL-8 concentration that move at a slower speed, which could give more insights into IL-8 receptor saturations and neutrophil desensitization pathways.

We further looked into the different chemotactic indices of neutrophils, namely, the chemotactic index (C.I.) which measures cell movement toward the gradient direction (defined as $\Delta x/d$), the motility index (M.I.) which evaluates random cell movement (migration distance divided by the product of migration speed and time), and the effective chemotactic index (E.C.I.), which assesses cell movement directionally and randomly (E.C.I. = C.I. \times M.I.). Definition of each index is detailed in the “Experimental Section” and Table S1 in the Supporting Information.

As shown in Figure 4c, both control groups show similar C.I., with a value close to zero. Neutrophils in the control regions migrated over short distances, but their average Δx value was zero (Figure 3c). In addition, the positive control group had a greater net displacement than the negative control group (Figure 3d), reflected by a higher M.I.

Collectively, these results are consistent with activation and random migration of cells within the positive control group. The C.I. and E.C.I. of the gradient groups are significantly

higher than cells in both control groups, indicating that neutrophils exposed to the concentration gradient effectively and actively moved in the direction of the gradient. Further, the chemotactic index of migrating neutrophils is well correlated to their initial position within the gradient, where neutrophils starting from the low end of the gradient show higher chemotactic responses (Figure 4d).

As a control, neutrophils were exposed to a concentration gradient of only Fluorescein Isothiocyanate-Dextran (FITC-Dextran), without IL-8, and did not show directed migration (Figure S6 in the Supporting Information). These experiments demonstrated that the exposure to the dextran solution did not influence neutrophil activation or migration. Further, 3D simulation results showed that the applied shear stresses within the gradient vary between zero at the stagnation point (SP, the center point) and a maximum value of 16×10^{-3} Pa under the edge of each aspiration aperture (Figure S1 in the Supporting Information). We analyzed the response of individual neutrophils that were exposed to different ranges of shear stresses within the gradient (see Figures S7 and S8 in the Supporting Information), and no significant difference was found, indicating

that the applied values of the shear stresses do not influence the neutrophil chemotactic response (see the Supporting Information for more details). However, a number of prior studies reported the effect of shear stress on various leukocytes^[37] and hematopoietic stem cells.^[38] Nonetheless, these studies applied significantly higher shear stresses than what we are applying to neutrophils in this study, and hence future studies using this setup could be directed toward evaluating the threshold at which shear stress influences neutrophil migration.

2.4. Neutrophil Chemotaxis in Moving IL-8 Concentration Gradients

The response of neutrophils to a moving IL-8 gradient was tested by manually displacing the MFP by $10 \mu\text{m}$ every 200 s (Figure 5a) corresponding to $0.05 \mu\text{m s}^{-1}$, in the direction of high IL-8 concentration. The floating gradient was thus moving in the same direction as migrating neutrophils. We selected this speed to approximately match with the average velocity of neutrophils in static gradients ($\approx 0.06 \mu\text{m s}^{-1}$). This allowed

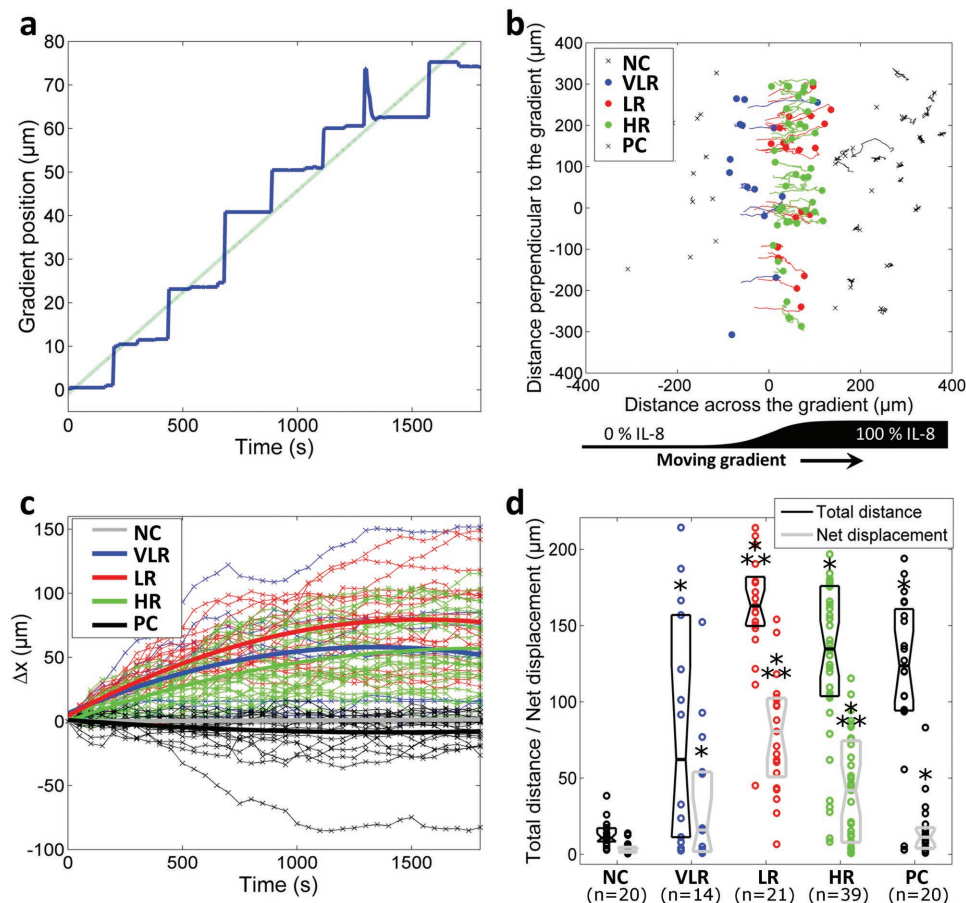


Figure 5. Neutrophil migration under moving IL-8 gradient. a) Position of the stagnation point, within the gradient, as a function of time showing the stepping motion with $10 \mu\text{m}$ steps. The linear fit has a slope of $0.054 \mu\text{m s}^{-1}$. b) Tracks of neutrophils from both control groups (NC and PC) and the gradient groups (VLR, LR, and HR). c) Migration distance (Δx) of total 114 individual neutrophils (thin lines) and second-order polynomial fit of the average displacement (thick lines) for each group of neutrophils as a function of time for all tracks shown in panel (b). d) Total distance and net displacement for each group under a moving gradient. Each open circle is the result of an individual neutrophil, and n is the total number of neutrophils analyzed in each group, from three separate experiments. Boxplots show the median and the first and third quartiles for each group. Single star (*) indicates p -value < 0.05 when compared to NC, and double stars (**) indicates p -value < 0.05 when compared to PC (t -test).

for simple tracking of neutrophil migration, while the stepping displacement of the MFP was accurate within 10% and could be completed in ≈ 5 s, although it carried risk of error as illustrated by the missed step at the end of the displacement trace (Figure 5a). Future automation of the gradient movement can be easily achieved by programming the motorized microscope stage in a closed-loop system, where cell displacement can be continuously tracked using the microscope and a real time image-processing algorithm to provide feedback positioning information to the stage, so the gradient can be moved accordingly.^[24]

Tracks of individual neutrophils (Figure 5b) were extracted for 1800 s from the time-lapse images (Video S5 in the Supporting Information). No difference was noted for neutrophils in the positive and negative control areas compared to stationary gradients. Some neutrophils from the VLR started migrating but then stopped, which was not observed in the static gradient. Based on the time-lapse images, we concluded that these neutrophils sensed the gradient, and started moving toward the high concentration, but could no longer sense the gradient as it was displaced and thus stopped migrating. These results suggest that neutrophils can rapidly lose their activation when they have only been stimulated at low concentration for a short time. Conversely, neutrophils from LR and HR migrated over longer distances compared to stationary gradients, possibly due to a delay of saturation effects.

The net displacement of individual neutrophils in the gradient direction over time is shown in Figure 5c and in Figure S9 in the Supporting Information, where neutrophils from the gradient groups showed significant net displacement with the moving gradient. Compared to stationary gradients (Figure 3c), neutrophils under moving gradients showed higher heterogeneity in their response (Figure 5d), and a higher proportion of neutrophils (38.9%) migrated longer than the gradient width (i.e., 75 μm). Moreover, neutrophils from HR showed higher net displacement, with 26.9% of neutrophils migrating further than the gradient width compared to 0% under the stationary gradient (Figure 3c). In addition, the net displacement of individual neutrophils was independent from their initial position within gradient ($R^2 = 0.012$, Figure S10 in the Supporting Information) in contrast to the stationary gradient experiments ($R^2 = 0.43$, Figure S5 in the Supporting Information).

Neutrophils from the HR in a stationary gradient (Figure 3c) only migrated a limited distance before reaching the constant concentration zone, while they migrated longer in a moving gradient (Figure 5c). The net displacement in LR and HR was significantly larger under the moving gradient when compared to the stationary gradient (p -values < 0.01), with 39.1% of neutrophils migrating beyond one gradient width when exposed to the moving gradient, compared to only 4.1% exposed to the stationary gradient (Figure S10 in the Supporting Information). These results indicate that neutrophils sense and follow a moving gradient, leading to longer migration than under static gradient conditions. Neutrophils in the negative and positive control groups responded similarly to stationary gradients regarding average speed and lack of directional migration (Figure 6a,b).

Akin to chemotaxis within the stationary gradients, neutrophils exposed to the moving gradients started migration at a

maximum velocity that diminished over time (Figure 5c). While the initial chemotaxis velocities are similar for stationary and moving gradients, cells in stationary gradients slowed down to below $0.02 \mu\text{m s}^{-1}$ at $t = 800$ s (Figure 4b), while for moving gradients it took 900 s for the VLR and 1350 s for LR and HR to reach this threshold (Figure 6b). Analogous to the stationary conditions, neutrophils from the LR group had the highest C.I. (Figure 6c). In contrast to the stationary case, the migration response under a moving gradient is not significantly different for neutrophils in different groups (Figure 6d). Summary of single cells' responses, under stationary and moving gradients, is shown in Table 1.

3. Discussion and Conclusions

By challenging neutrophils with stationary and moving IL-8 concentration gradients, we were able to observe differences at the single cell level, and neutrophils were shown to migrate longer under moving gradients. The results revealed that the chemotactic response of neutrophils is dependent on their initial position within a stationary gradient, which is consistent with the concept of rapid neutrophil desensitization. However, this dependency diminished under moving gradients, where a higher fraction of neutrophils migrated for distances longer than the initial gradient width. In both gradient modes, neutrophils were shown to start their migration at the highest speeds and then gradually slow down before stopping, with the rate of slowing being higher in stationary gradients. The open nature of the MQ permitted for precise control of exposing neutrophils to gradients and allowed for measuring the accurate neutrophil response time (30 s). Suspended neutrophils, carried by the fluid flow, attached to the pristine dish upon entering the gradient, and high-magnification imaging and velocity analysis suggested a rolling-like behavior on the substrate before attaching. This suggests an IL-8 receptor-dependent mechanism for rapid cell adhesion upon entering the gradient region in a rolling-like behavior. Neutrophils were shown to be responsive, quick in detecting the gradient's plateau, and to rapidly become unresponsive when exposed to low IL-8 concentration for short periods, suggesting quick receptor saturation and/or desensitization mechanisms.

Our work complements the study on neutrophils on a microfluidic treadmill by Irimia and co-workers,^[24] where a feedback controller was used to hold an individual migrating neutrophil in same place within a LTB_4 concentration gradient. The study uses a "multifunctional microfluidic pipette,"^[39] which also generates a gradient, but with slower response time and less control than the MFP in the absence of a cover; indeed, the Hele-Shaw configuration of the MFP creates a stronger flow confinement^[40,41] allowing for steeper and more rapid gradient formation and movements. The use of a continuously moving substrate however allows us to continuously position a migrating single cell at a particular spot within the gradient, and also study the separate effect of temporal and spatial concentration gradients on migration. While our study did not consider the isolated effect of temporal and spatial gradients, this can be performed in the future by including a feedback controller to hold a single migrating cell in the same

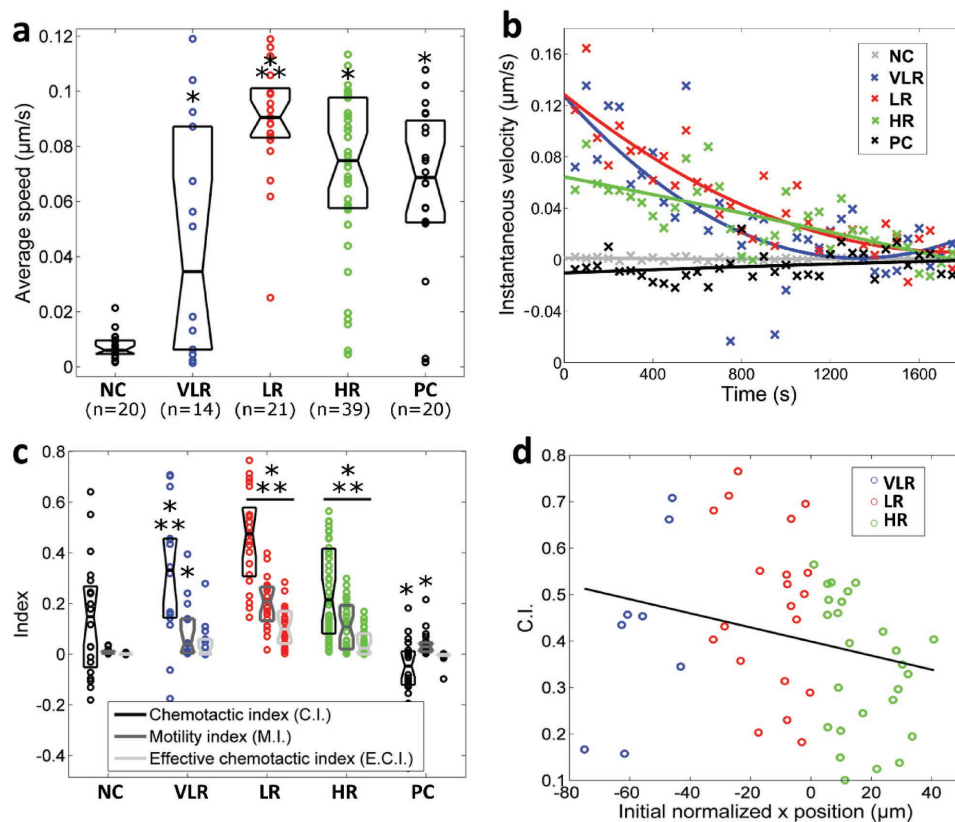


Figure 6. Migration and motility analysis of neutrophils in moving IL-8 concentration gradient. a) Average cell migration speed for each group. n is the total number of neutrophils analyzed in each group, from three separate experiments. b) Average instantaneous migration velocity in the gradient direction for each cell group. c) The C.I., M.I., and E.C.I. for each group. d) The C.I. as a function of initial cell position along the gradient ($R^2 = 0.06$). Each open circle “○” represents an individual neutrophil and the cross “×” represents the group averaged value for each 50 s period while lines are fitted averages. n is the total number of neutrophils in each group. Boxplots show the median and the first and third quartiles for each group. Single star (*) indicates p -value < 0.05 when compared to NC, and double stars (**) indicates p -value < 0.05 when compared to PC (t -test).

spot within the gradient. While both studies find that neutrophil response differs between static and moving gradients, in this work we observed longer migrations in moving gradients of IL-8, whereas in the treadmill experiments, migration length in response to a moving gradient of LTB₄ was reduced. This difference is likely due to one of two factors, or both. First, in this study the gradient movement speed was fixed (based on the average velocity of all neutrophils in static gradients) and not matched to a single cell migration speed in real time, thus potentially leading to changes in neutrophil position within the gradient (combined effect of spatial and temporal gradients). However, the treadmill experiments maintained a neutrophil at the same position within the gradient and thus the cell senses a

constant gradient (no temporal effect of the gradient included). Second, different chemotactic molecules and concentrations were used, one being a small protein (IL-8) and the other being a leukotriene, and thus the relative sensitivity of neutrophils to each molecule is likely different.

Future experiments can also consider moving gradients with different speeds and concentrations, in the forward direction, in the backward direction (gradient movement against the direction of migration), or both, which could help in studying desensitization mechanisms. Moreover, interesting extension of this work can be utilized to study neutrophil rolling, tether-to-sling transitions,^[18] and polarization on substrates coated with extracellular matrix, cell adhesion molecules, or a monolayer of endothelial cells culture.^[20] Other future work could include experiments with higher value of applied shear stresses that could represent physiological values,^[42] different chemokines and concentrations, and higher number of neutrophils. These experiments may help in understanding neutrophil recruitment and trafficking in dynamic environments,^[7] and could open the door for developing effective and selective therapies for infections and inflammation. Moreover, this setup can be used atop of patterned surfaces to study the combined chemotactic and haptotactic responses,^[43] or in a chamber out-fitted with electrodes to study the effect of electrotaxis.^[44]

Table 1. Net displacement (Δx) in the direction of the gradient and the average migration speed (\bar{v}) of single cells under stationary and moving gradients. Mean \pm standard deviation are displayed.

		VLR	LR	HR
Δx [μm]	Stationary	59.3 \pm 25	42.5 \pm 24.4	18.4 \pm 9.3
	Moving	59.8 \pm 47.3	82.8 \pm 34.8	59.6 \pm 29.2
\bar{v} [$\mu\text{m min}^{-1}$]	Stationary	4.1 \pm 3.4	5.9 \pm 1.9	4.3 \pm 1.5
	Moving	2.7 \pm 2.5	5.4 \pm 1.3	4.3 \pm 1.7

This work proposes a new framework in the field of cell chemotaxis, by using moving concentration gradients that may better represent in vivo conditions. Collectively, our results showed neutrophils' extended migration in response to moving gradients, but only to a limited extent, presumably because of desensitization^[45] or memory effects.^[17] In vivo concentration gradients of IL-8 are host produced (e.g., macrophages and epithelial cells), and it would be of interest to study gradients of pathogen-derived chemokines (e.g., fMLP) and monitor cell navigation and tracking. This work illustrates the functionality and potential of the moving gradients to study neutrophils, and other stimuli-responsive cells, at the single cell level, to measure polarization, migration, desensitization, and other mechanisms, such as cell rolling and arrest behavior on substrates, and their associated signaling pathways. This study focused on one cue at one concentration, and used gradient displacement in a single direction at one velocity. The parameters space, including cue, gradient steepness and slope, speed, and direction, is huge, and can be further expanded by changing the substrate (prepatterned, soft, 3D) and by including additional cues, highlighting the need for further experiments and new approaches. Various types of cells may be challenged with moving gradients and may help uncover new facets of cell chemotaxis not observable under static gradient conditions.

4. Experimental Section

Neutrophil Isolation, Purification, and Labeling: Blood was obtained from three healthy volunteers after informed consent, and collected in BD Vacutainer Heparin Blood Collection Tubes. This study was performed in agreement with the ethical review board of McGill University and the Research Institute of the McGill University Health Center (permission # B-07435). Neutrophil isolation was achieved by density gradient centrifugation (Mono-Poly Resolving Medium, MP Biomedicals, 1698049); see details in Figure S2 and in the Supporting Information. Neutrophils were then stained with eFluor670-proliferation dye (eBiosciences, 5 μL , 5×10^{-3} M), and up to 10×10^6 cells were re-suspended in 1 mL of complete RPMI 1640 culture medium (Invitrogen, CA), supplemented with 10% heat-inactivated fetal bovine serum (FBS), penicillin (100 U mL^{-1}), streptomycin (100 $\mu\text{g mL}^{-1}$), 2×10^{-3} M L-glutamine, 10×10^{-3} M 4-(2-hydroxyethyl)-1-piperazineethanesulfonic acid (HEPES), 0.1×10^{-3} M nonessential amino acids, 1×10^{-3} M sodium pyruvate (Invitrogen Life Technologies, Carlsbad, CA, USA), and 50×10^{-6} M 2-ME (Sigma-Aldrich, St. Louis, MO, USA). Neutrophils were subsequently incubated for 5 min at 37 °C and washed three times with phosphate-buffered saline (PBS) supplement with 10% FBS. Neutrophils were then seeded within Petri dishes and left at least for 1 h in the incubator before starting the chemotaxis experiments, and experiments were performed within 8 h of blood withdrawal.

Preparation of the Interleukin-8 Solution: Solutions of IL-8 ($M_w = 8$ kDa, Sigma, MO) were diluted in RPMI 1640 medium (Invitrogen, CA) with 10% FBS (Sigma, MO) to a final concentration of 25 ng mL^{-1} . FITC-Dextran (Sigma-Aldrich) with a molecular weight of 10 kDa was added to the IL-8 solution as a fluorescent indicator for the generated concentration gradient of IL-8. IL-8 solutions were freshly prepared right before setting up the experiments.

The MQ and Floating Gradients: The floating concentration gradient of IL-8 was generated within the MQ. The MQ was formed under an MFP with four apertures arranged at the corners of a virtual square. The MFP was assembled as a square Silicon chip (3 mm in width) with four holes of 360 μm diameter serving as the fluidic apertures, and a polydimethylsiloxane (PDMS) interface chip for connecting glass capillaries (200 μm ID and 360 μm OD, Polymicro Technologies,

Phoenix, AZ) to the apertures. Capillaries were connected to prefilled glass syringes (Hamilton, Reno, NV) driven by syringe pumps (Nemesys Cetoni, Korbussen, Germany) via NanoTight connectors (Upchurch Scientific, Oak Harbor, WA). Prior to the experiment, the MFP was mounted on an XYZ micropositioner and positioned in close proximity and parallel to the neutrophil-containing dish on the automated microscope stage (PZ-2000 microscope stage, Applied Scientific Instrumentation, Eugene, OR) of the inverted microscope (TE2000, Nikon, Saint-Laurent, QC, Canada). The micropositioner was controlled manually in the XY-plane with two orthogonal linear stages and micrometer screws (M-443-4 and SM-50, Newport Corporation, Fountain Valley, CA), and the Z-axis positioning was automatically controlled using a high-resolution linear stage (LS-50 linear stage, Applied Scientific Instrumentation, Eugene, OR). Experiments started with simultaneous injections and aspirations through the MQ's apertures in the gap between the MFP and the neutrophil-containing dish. Consequently, the MQ was generated with an SP in its center. Following the injection of a chemokine through one of the poles, the concentration gradient was formed across the SP and fluidic interface. Details of the experimental setup and the concentration gradient generation were explained in the previous work.^[25] As the gradient was formed in the gap between the MFP and the bottom dish, it was termed as "floating" since confined between two plates in an open microfluidic system. The open nature of the setup allowed for moving the gradient from one area of interest to another at any time during the experiment. For all of the work described in this manuscript, the gap between the two plates was 50 μm , the injection flow rate was 3 nL s^{-1} , and the aspiration flow rate was 10 nL s^{-1} . For all of chemotaxis experiments, temperature was maintained at 37 °C and humidity at 70% within an environmental chamber (Precision Plastics, Inc.) mounted on the microscope.

Image Acquisition and Time-Lapse Microscopy: A cooled CCD camera (Photometrics CoolSNAP HQ2) was connected to the fluorescent microscope and images were recorded with 10 \times (Nikon, numerical aperture (NA) = 0.3), 20 \times (Nikon, NA = 0.45), and 40 \times (Nikon, NA = 0.6) objectives. Time-lapse images of the gradient and neutrophils were independently captured every 5 s for the duration of the experiment, and the two fluorescent channels were merged using the NIS-Elements imaging software (Nikon, Saint-Laurent, QC, Canada). Exposure times for the red and green filters were 500 and 200 ms, respectively.

Characterization of the Concentration Gradients: Time-lapse images were analyzed using a homemade code in MATLAB (v 8.0, The MathWorks, Inc., MA) to calculate the position of the SP, the generated gradient width, and to distinguish neutrophils within different groups with respect to their initial position within the gradient. More details are shown in Figure S11 of the Supporting Information. Neutrophils within the gradient were arbitrarily assigned to three categories depending on their initial position within the gradient, which were called the gradient groups. Neutrophils located at the low end of the gradient below the 10% range (<2.5 ng mL^{-1} IL-8) were termed as VLR group. Neutrophils located in the area between 10% and 50% (2.5–12.5 ng mL^{-1} IL-8) were termed LR group, while the ones between 50% and 90% (12.5–22.5 ng mL^{-1} IL-8) were called HR group. In addition, two control groups were defined as the negative control group for neutrophils in the area without IL-8 and positioned far from the gradient, and the positive control group for neutrophils located in the area perfused by the maximal concentration of IL-8; see Figure S3 in the Supporting Information. Gradient stability was evaluated by examining relative intensity and gradient width at the SP with respect to time during the experiment. Relative intensities of each acquired gradient frame were normalized so that 0 corresponded to the minimum (0% IL-8) gradient intensity value and 1 corresponded to the maximum (100% IL-8) gradient intensity value. Gradient width was defined as the distance between the 10% and 90% values of the fluorescent signal at the SP. The time zero was defined as the first acquired frame once the MQ was activated. The gradient took ≈ 40 s to stabilize after activation of the fluid flow (Figure 1e).

Analysis of Neutrophil Response: The time-lapse images of each experiment were imported into ImageJ 1.42 (National Institutes of

Health, MD), and the migration response of individual cells was tracked using the MTrackJ plugin.^[46] The position of the center of each neutrophil was tracked over periods of 50 s, and data were then exported for further analysis into MATLAB (v 8.0, The MathWorks, Inc., MA). The raw data were then normalized so that the gradient direction was aligned with the x-axis, and the SP represented the center point (0, 0); see Figure S11 in the Supporting Information. Next, four important parameters were calculated for individual cells as the following: 1) the total travelled distance “*d*” which is defined as the length of the migration path over the course of the experiment, 2) the displacement vector “*r*”, which is defined as the migration distance in total, 3) the net displacement “ Δx ” which is defined as the migration distance in the direction of the gradient, and 4) the average cell migration speed which is defined as the total travelled distance divided by total time “ $s = d/t$ ”; see Table S1 (Supporting Information) for more details.

Afterward, the C.I., the M.I., and the E.C.I. of neutrophils in the different groups were calculated. The C.I. evaluates the proportion of a cell's total displacement that contributes to a net displacement in the increasing gradient direction. The M.I. measures the effectiveness and activeness of a neutrophil's movement in any direction. The E.C.I. is similar to the C.I., but also takes into account the activeness of the cell. For example, a cell that moves only slightly in a gradient's direction would have a high C.I., but a fairly low E.C.I. More details are given in Table S1 (Supporting Information). These parameters were calculated for every individual neutrophil located within the gradient groups (VLR, LR, and HR). When only migrating cells were to be analyzed, a threshold was applied based on the M.I. of individual neutrophils and subsets of the data for the gradient groups were obtained. The threshold was applied to data shown in Figures 4d and 6d, and in Figures S4, S5, S9, and S10 in the Supporting Information. Neutrophils that had an M.I. comparable to the ones in the negative control (*p*-value > 0.95) were considered unresponsive and thus eliminated.

Sample Size and Statistical Analysis: For cell polarization and rolling studies, results represented *n* = 9 individual neutrophils from two separate experiments, while results analyzing the time for cells to initiate migration represented *n* = 36 individual neutrophils from three separate experiments. Results extracted from stationary and moving gradients, for all gradient and control groups, represented *n* = 214 and *n* = 114 neutrophils, respectively, from three separate experiments each. An exact number of neutrophils for each gradient and control group are shown under the x-axis in Figures 3d and 5d, respectively. Data were graphically represented as a scatterplot overlaid to a standard boxplot, showing the median as well as first and third quartiles. The notches indicate $\pm 1.57 \times \text{IQR} / \sqrt{n}$, where IQR is the interquartile range and *n* is the number of neutrophils in each group. When comparing two groups, a two-tailed *t*-test was performed in MATLAB (v 8.0, The MathWorks, Inc., MA), assuming equal or unequal variances depending on the result of an *F*-test. Data reported with the plus-minus uncertainty values represent data average \pm standard deviations.

Numerical Simulations: 3D simulations (Figure S1 in the Supporting Information) were carried out using COMSOL Multiphysics 3.5 (commercially available finite element simulation software). Simulations coupled the solutions of the Navier–Stokes equation and convection–diffusion equation. Sample solutions were assumed to be incompressible Newtonian fluids with a density of 1000 kg m⁻³, and a dynamic viscosity of 0.001 N s m⁻² (water). The diffusion coefficient of the interleukin-8 in water was set to 210 μm² s⁻¹.^[47] The simulations were run under steady-state conditions and assumed no-slip boundary conditions on walls, with the flow boundary conditions set as open boundaries. The injection and aspiration flow rates in the simulations were set to 3 and 10 nL s⁻¹, respectively, which matched experimental values. The concentration of the interleukin-8 at the source injection aperture was arbitrarily set to 1 and 0 mol m⁻³ at the other injection aperture.

Supporting Information

Supporting Information is available from the Wiley Online Library or from the author.

Acknowledgements

The authors acknowledge funding from NSERC, CIHR, CHRP, Genome Canada, Genome Quebec, and CFI. The authors thank Dr. Eva d'Hennezel and Dr. Sebastian Leathersich for technical assistance. M.A.Q. acknowledges financial support from New York University Abu Dhabi, and M.P. acknowledges financial support from CIHR Frederick Banting and Charles Best Canada Graduate Scholarships and Doctoral awards. S.M.V. and D.J. acknowledge support from Canada Research Chair program. M.A.Q. and D.J. designed the research. M.A.Q. performed the experiments. M.P. and S.M.V. isolated, purified, and labeled human neutrophils. M.A.Q., M.A., and D.J. analyzed the results. M.A.Q. and D.J. wrote the manuscript. M.P., M.A., and S.M.V. edited the manuscript.

Conflict of Interest

The authors declare no conflict of interest.

Keywords

chemotaxis, concentration gradients, microfluidic quadrupole, microfluidics, neutrophils

Received: December 11, 2017

Revised: March 11, 2018

Published online:

- [1] a) E. Kolaczowska, P. Kubers, *Nat. Rev. Immunol.* **2013**, *13*, 159; b) B. Amulic, C. Cazalet, G. L. Hayes, K. D. Metzler, A. Zychlinsky, *Annu. Rev. Immunol.* **2012**, *30*, 459.
- [2] a) M. McCutcheon, *Physiol. Rev.* **1946**, *26*, 319; b) M. McCutcheon, *Ann. N. Y. Acad. Sci.* **1955**, *59*, 941.
- [3] a) S. Boyden, *J. Exp. Med.* **1962**, *115*, 453; b) S. H. Zigmond, *Nature* **1974**, *249*, 450; c) S. H. Zigmond, *J. Cell Biol.* **1977**, *75*, 606; d) D. Zicha, G. A. Dunn, A. F. Brown, *J. Cell Sci.* **1991**, *99*, 769.
- [4] G. Gerisch, H. U. Keller, *J. Cell Sci.* **1981**, *52*, 1.
- [5] W.-J. Rappel, L. Edelstein-Keshet, *Curr. Opin. Syst. Biol.* **2017**, *3*, 43.
- [6] P. J. M. Van Haastert, P. N. Devreotes, *Nat. Rev. Mol. Cell Biol.* **2004**, *5*, 626.
- [7] A. Chandrasekaran, F. Ellett, J. Jorgensen, D. Irimia, *Microsyst. Nanoeng.* **2017**, *3*, 16067.
- [8] S. de Oliveira, E. E. Rosowski, A. Huttenlocher, *Nat. Rev. Immunol.* **2016**, *16*, 378.
- [9] a) T. E. Van Dyke, C. Wilson-Burrows, S. Offenbacher, P. Henson, *Infect. Immun.* **1987**, *55*, 2262; b) M. W. N. Harbord, D. J. B. Marks, A. Forbes, S. L. Bloom, R. M. Day, A. W. Segal, *Aliment. Pharmacol. Ther.* **2006**, *24*, 651.
- [10] O. D. Weiner, G. Servant, M. D. Welch, T. J. Mitchison, J. W. Sedat, H. R. Bourne, *Nat. Cell Biol.* **1999**, *1*, 75.
- [11] W. S. Ramsey, *Exp. Cell Res.* **1972**, *70*, 129.
- [12] a) D. Irimia, *Annu. Rev. Biomed. Eng.* **2010**, *12*, 259; b) X. Wang, Z. Liu, Y. Pang, *RSC Adv.* **2017**, *7*, 29966.
- [13] N. Li Jeon, H. Baskaran, S. K. W. Dertinger, G. M. Whitesides, L. Van De Water, M. Toner, *Nat. Biotechnol.* **2002**, *20*, 826.
- [14] E. K. Sackmann, E. Berthier, E. W. K. Young, M. A. Shelef, S. A. Remington, A. Huttenlocher, D. J. Beebe, *Blood* **2012**, *120*, e45.
- [15] D. Irimia, S.-Y. Liu, W. G. Tharp, A. Samadani, M. Toner, M. C. Poznansky, *Lab Chip* **2006**, *6*, 191.
- [16] F. Lin, C.-C. Nguyen, S.-J. Wang, W. Saadi, S. Gross, N. Jeon, *Ann. Biomed. Eng.* **2005**, *33*, 475.

- [17] K. Yang, J. Wu, G. Xu, D. Xie, H. Peretz-Soroka, S. Santos, M. Alexander, L. Zhu, M. Zhang, Y. Liu, F. Lin, *Integr. Biol.* **2017**, *9*, 303.
- [18] A. Marki, E. Gutierrez, Z. Mikulski, A. Groisman, K. Ley, *Sci. Rep.* **2016**, *6*, 28870.
- [19] E. Reátegui, F. Jalali, A. H. Khankhel, E. Wong, H. Cho, J. Lee, C. N. Serhan, J. Dalli, H. Elliott, D. Irimia, *Nat. Biomed. Eng.* **2017**, *1*, 0094.
- [20] X. Wu, M. A. Newbold, Z. Gao, C. L. Haynes, *Biochim. Biophys. Acta, Gen. Subj.* **2017**, *1861*, 1122.
- [21] S. F. Moussavi-Harami, K. M. Mladinich, E. K. Sackmann, M. A. Shelef, T. W. Starnes, D. J. Guckenberger, A. Huttenlocher, D. J. Beebe, *Integr. Biol.* **2016**, *8*, 243.
- [22] a) F. Wang, *Cold Spring Harbor Perspect. Biol.* **2009**, *1*, a002980; b) M. Phillipson, P. Kubes, *Nat. Med.* **2011**, *17*, 1381.
- [23] T. M. Keenan, C. W. Frevert, A. Wu, V. Wong, A. Folch, *Lab Chip* **2010**, *10*, 116.
- [24] A. J. Aranyosi, E. A. Wong, D. Irimia, *Lab Chip* **2015**, *15*, 549.
- [25] M. A. Qasaimeh, T. Gervais, D. Juncker, *Nat. Commun.* **2011**, *2*, 464.
- [26] M. A. Qasaimeh, S. G. Ricoult, D. Juncker, *Lab Chip* **2013**, *13*, 40.
- [27] S. H. Zigmund, S. J. Sullivan, *J. Cell Biol.* **1979**, *82*, 517.
- [28] a) A. D. Zadeh, H. Keller, *Eur. J. Cell Biol.* **2003**, *82*, 93; b) H. U. Keller, A. Zimmermann, *Biomed. Pharmacother.* **1987**, *41*, 285.
- [29] B. C. Chesnutt, D. F. Smith, N. A. Raffler, M. L. Smith, E. J. White, K. Ley, *Microcirculation* **2006**, *13*, 99.
- [30] A. F. H. Lum, C. E. Green, G. R. Lee, D. E. Staunton, S. I. Simon, *J. Biol. Chem.* **2002**, *277*, 20660.
- [31] M. L. Smith, T. S. Olson, K. Ley, *J. Exp. Med.* **2004**, *200*, 935.
- [32] G. E. Rainger, A. C. Fisher, G. B. Nash, *Am. J. Physiol.* **1997**, *272*, H114.
- [33] R. E. Gerszten, E. A. Garcia-Zepeda, Y.-C. Lim, M. Yoshida, H. A. Ding, M. A. Gimbrone, A. D. Luster, F. W. Luscinskas, A. Rosenzweig, *Nature* **1999**, *398*, 718.
- [34] J. A. DiVietro, M. J. Smith, B. R. E. Smith, L. Petruzzelli, R. S. Larson, M. B. Lawrence, *J. Immunol.* **2001**, *167*, 4017.
- [35] a) K. Ley, C. Laudanna, M. I. Cybulsky, S. Nourshargh, *Nat. Rev. Immunol.* **2007**, *7*, 678; b) A. Zarbock, K. Ley, R. P. McEver, A. Hidalgo, *Blood* **2011**, *118*, 6743.
- [36] E. J. Kunkel, J. L. Dunne, K. Ley, *J. Immunol.* **2000**, *164*, 3301.
- [37] M. P. Valignat, O. Theodoly, A. Gucciardi, N. Hogg, A. C. Lellouch, *Biophys. J.* **2013**, *104*, 322.
- [38] A. Buffone, N. R. Anderson, D. A. Hammer, *J. Cell Sci.* **2018**, *131*, jcs205575.
- [39] A. Ainla, G. D. Jeffries, R. Brune, O. Orwar, A. Jesorka, *Lab Chip* **2012**, *12*, 1255.
- [40] A. Ainla, G. Jeffries, A. Jesorka, *Micromachines* **2012**, *3*, 442.
- [41] A. T. Brimmo, M. A. Qasaimeh, *RSC Adv.* **2017**, *7*, 51206.
- [42] T. G. Papaioannou, C. Stefanadis, *Hell. J. Cardiol.* **2005**, *46*, 9.
- [43] J. Roy, J. Mazzaferri, J. G. Filep, S. Costantino, *Sci. Rep.* **2017**, *7*, 2869.
- [44] Y.-S. Sun, *Sensors* **2017**, *17*, 2048.
- [45] H. Ali, R. M. Richardson, B. Haribabu, R. Snyderman, *J. Biol. Chem.* **1999**, *274*, 6027.
- [46] E. Meijering, O. Dzyubachyk, I. Smal, in *Methods in Enzymology* (Ed: P. M. Conn), Vol. 504, Academic Press, San Diego, CA **2012**, p. 183.
- [47] C. W. Frevert, G. Boggy, T. M. Keenan, A. Folch, *Lab Chip* **2006**, *6*, 849.

ADVANCED BIOSYSTEMS

Supporting Information

for *Adv. Biosys.*, DOI: 10.1002/adbi.201700243

Neutrophil Chemotaxis in Moving Gradients

Mohammad A. Qasaimeh, Michal Pyzik, Mélina Astolfi,
Silvia M. Vidal, and David Juncker**

Copyright WILEY-VCH Verlag GmbH & Co. KGaA, 69469 Weinheim, Germany, 2016.

Supporting Information

Neutrophil chemotaxis in moving gradients

*Mohammad A. Qasaimeh**, *Michal Pyzik*, *Mélina Astolfi*, *Silvia M. Vidal*, and *David Juncker**

Neutrophil purity. Neutrophil isolation was achieved by density gradient centrifugation (Mono-Poly Resolving Medium, MP Biomedicals, 1698049). To test for neutrophil purity, cells from fraction 1 and fraction 2 were stained with CD15-FITC (eBioscience, 11-0159-41), CD66b-APC (eBioscience, 17-0666-41), CD3-eFluor450 (BD-Biosciences, 560366), and CD14-PE (BD-Biosciences, 561707) antibodies according to the manufacturer's instructions. Our isolation consisted of above 97% neutrophils. Cells were acquired using BD FACS-Canto flow cytometer (BD Biosciences, Mississauga, ON, Canada), see Figure S2.

Analysis of time-lapse images. Time-lapse images of the gradient and neutrophils were independently captured every 5 s for the duration of the experiment. Images were then analyzed using a homemade MATLAB (v 8.0, The MathWorks, Inc., Massachusetts) code to calculate the position of the stagnation point and the gradient width, and to separate neutrophils within three different groups depending on their initial position within the gradient. For experiments with stationary gradients, all frames (time points) of the fluorescein channel acquired during an experiment were first averaged to compensate for inter-frame variations in gradient position and intensity. For a moving gradient, only the first frames (when the gradient was stationary) were averaged. On the averaged image, regions of 100% intensity and 0% gradient intensity as well as two lines across the concentration gradient direction near each of the MFP's two aspiration apertures were selected manually. The 50%

intensity points along the two lines were found and joined by a segment. The stagnation point position was found along this segment by determining the middle point between the manually selected edges of both aspirating apertures. Then, one hundred intensity profiles (uniformly distributed) were generated by the code across the gradient, perpendicular to the 50% intensity segment, and used to find the 10%, 50%, and 90% gradient intensity lines (See Figure S11). The gradient lines were drawn on the merged image of the cells and the concentration gradient.

Shear stress effect on migrating neutrophils. Neutrophils under the gradient were grouped based on their initial position (y-axis) with respect to the stagnation point (SP), in the center, to investigate the effect of shear stresses. Based on our simulation results (Figure S1), we divided the region between the aspiration apertures into three groups: Group 1 for areas within 119 μm of the SP in the vertical direction where neutrophils would be exposed to shear stresses less than 4×10^{-3} Pa, group 2 for areas at a distance of 119 to 238 μm from the SP in the vertical direction where neutrophils would be exposed to maximum shear stress of 8×10^{-3} Pa, and group 3 for areas at a distance of 238 to 357 μm from the SP in the vertical direction where neutrophils would be exposed to shear stresses below 16×10^{-3} Pa. These values of shear stresses are threefold lower than the physiologic range of the shear stresses measured in blood capillaries.^[42] Neutrophil tracks of the three vertical groups are shown in Figure S7. Analysis of the net displacement, E.C.I., and other indices (Figure S8) showed no significant difference between the three different regions of shear stresses. These results indicate that the applied values of the shear stresses do not influence neutrophils' chemotactic responses. These results are expected because of the low applied shear stresses in this setup compared to the *in vivo* values of shear stresses.

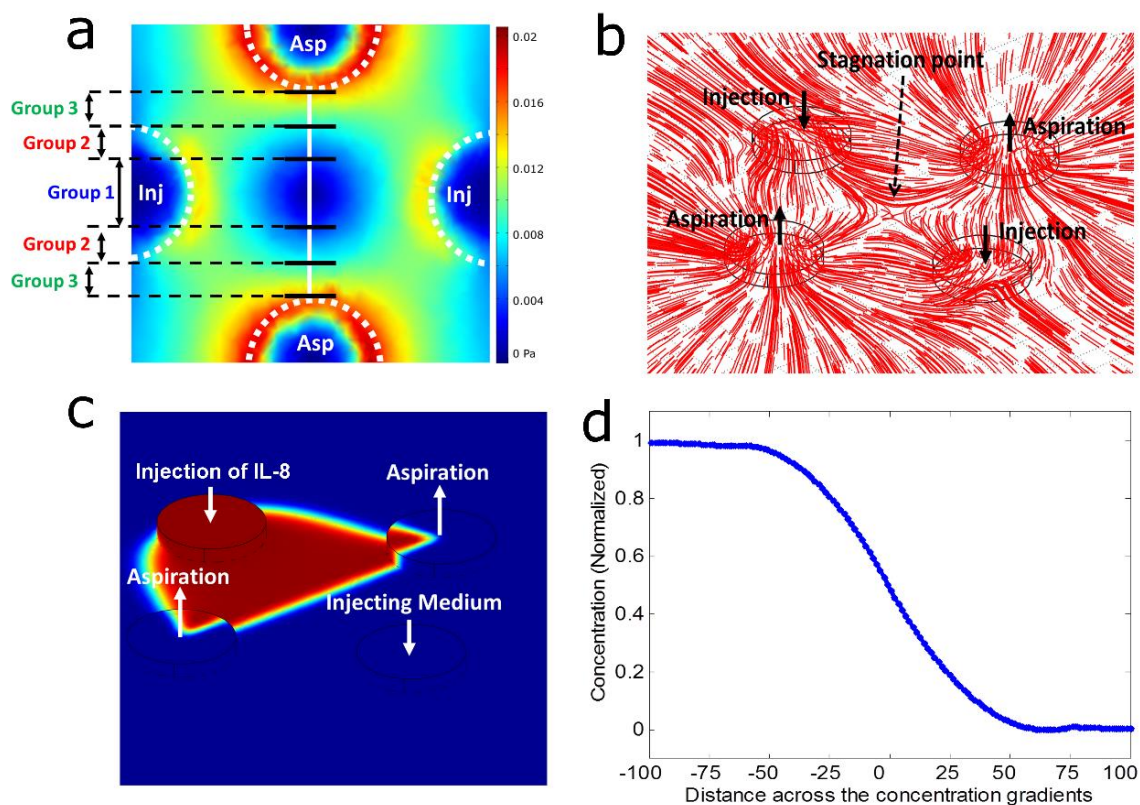


Figure S1. 3D simulation of the MQ and generated IL-8 concentration gradient. (a) A graph of the generated shear stresses on the bottom plate. The area between the inner edges of the aspiration apertures is divided into three sub-groups: group 1 for areas within $119 \mu\text{m}$ of the stagnation point in the vertical direction (average shear stress of approximately 2×10^{-3} Pa), group 2 for areas at a distance of 119 to $238 \mu\text{m}$ of the stagnation point in the vertical direction (average shear stress of approximately 6×10^{-3} Pa), and group 3 for areas at a distance of 238 to $357 \mu\text{m}$ of the stagnation point in the vertical direction (average shear stress of approximately 12×10^{-3} Pa). (b) 3D view of the flow stream lines, showing the stagnation point in the center of the MQ and the hydrodynamic confinements of injected fluids. (c) 3D view of the generated concentration gradients across the stagnation point and the injected fluids interface. (d) Concentration profile of the generated gradient across the stagnation point, showing a gradient width of $75 \mu\text{m}$. The gradient width is calculated as the distance between 90% and 10% of the maximum normalized concentration intensity.

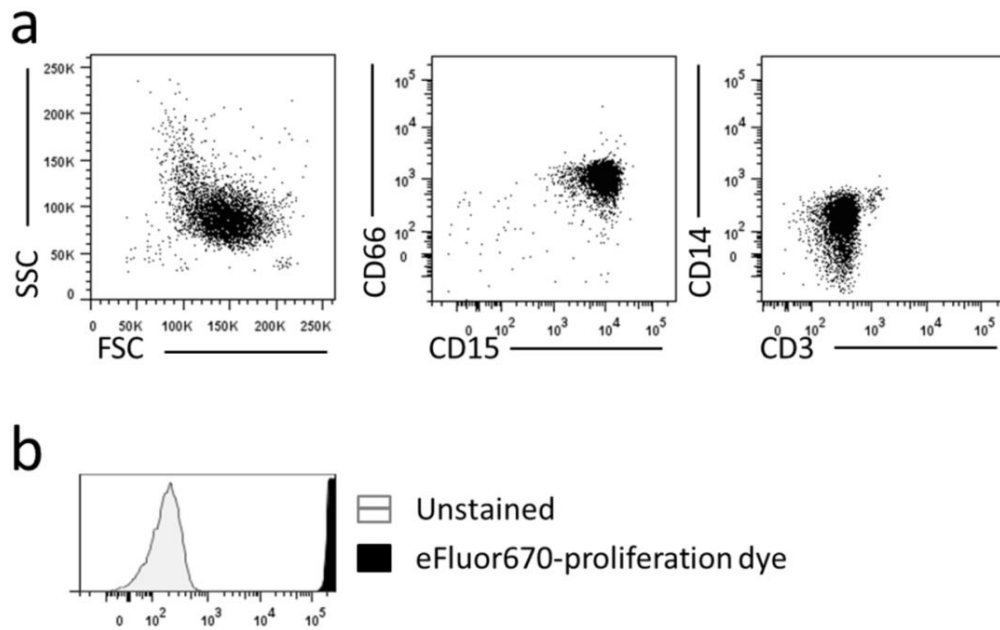


Figure S2. Isolated neutrophil purity. Polymorphonuclear leucocytes were isolated from the blood of healthy donors, and a small fraction was stained for Neutrophil (CD15, CD66b), Monocyte (CD14), and Lymphocyte (CD3) specific surface markers for purity assessment. (a) Representative dot plots are shown and demonstrate greater than 97% neutrophil recovery (CD15+, CD66b+, CD3-, CD14-) from one of several isolations performed. The remaining isolated cells were subsequently stained with eFluor670-proliferation dye. (b) Representative histogram of unstained and stained neutrophil fractions is shown.

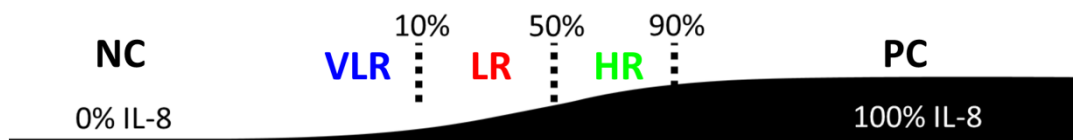


Figure S3. Neutrophils are categorized based on their initial position within the MQ. NC (negative control) for cells exposed to medium and PC (positive control) for cells exposed to 100% IL-8. Neutrophils within the gradient are classified as VLR (very low range) group for cells within 0%-10% of the gradient, LR (low range) group for cells within 10%-50% of the gradient, and HR (high range) group for cells within 50%-90% of the gradient.

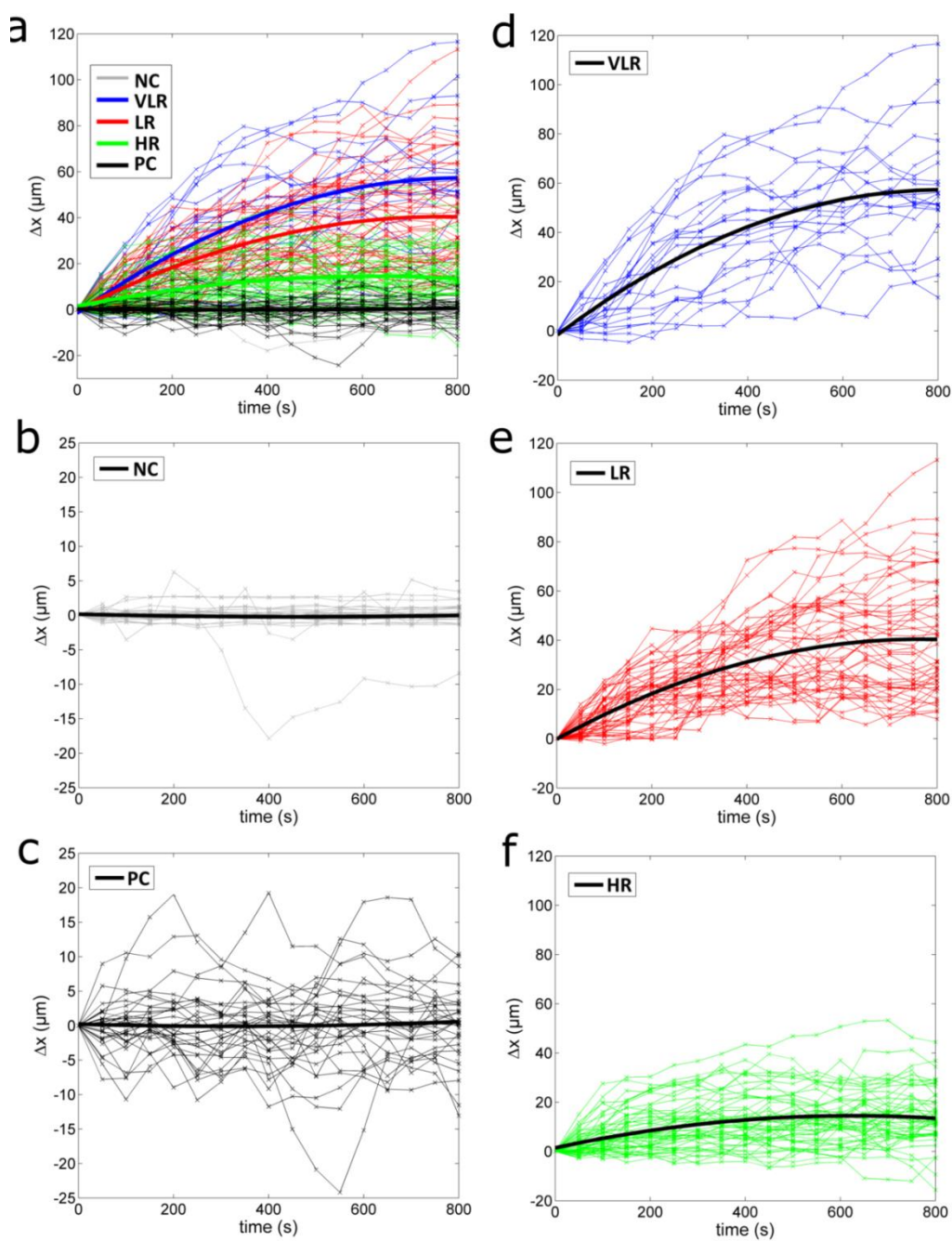


Figure S4. Analysis of individual neutrophils' migratory displacement under the stationary gradient with respect to time. (a) Neutrophils in all groups. (b) Neutrophils in the NC (negative control area). (c) Neutrophils in the PC (positive control area). (d) Neutrophils in the VLR group. (e) Neutrophils in the LR group. (f) Neutrophils in the HR group. Thick lines represent a second degree polynomial, fitting the averaged data for each group.

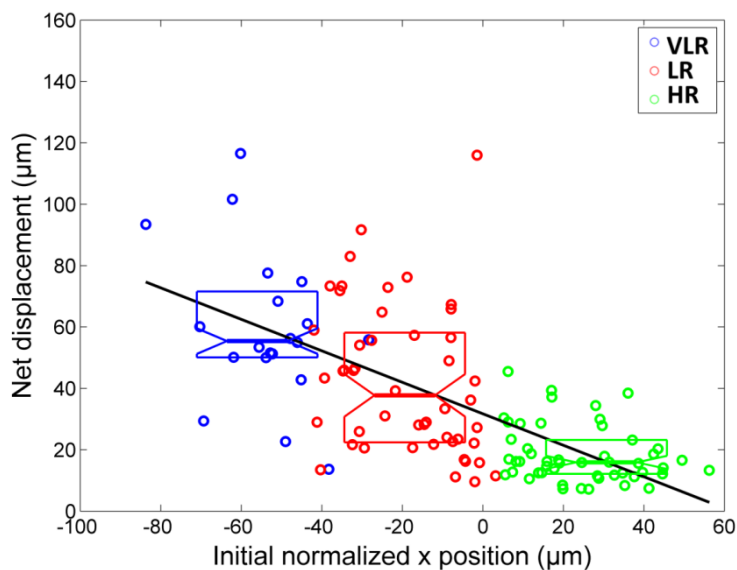


Figure S5. Neutrophils migration under a stationary concentration gradient of IL-8. Net displacement of migrating neutrophils is correlated ($R^2=0.43$) to their initial position within the stationary gradient.

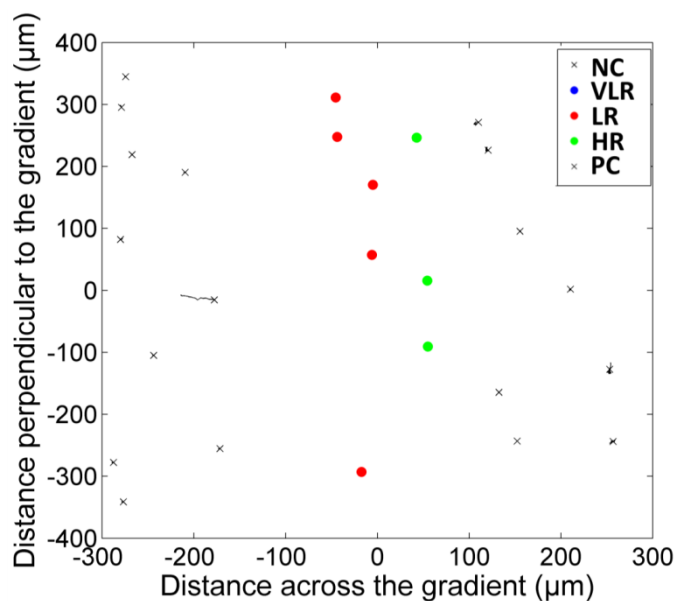


Figure S6. Neutrophil migration exposed to a false concentration gradient. Tracks of neutrophils exposed to a concentration gradient of FITC-Dextran (no IL-8) for 800 seconds. The tracks of the three regions (negative control (0% FITC-Dextran), positive control (100% FITC-Dextran), and gradient region) show no migratory response of neutrophils.

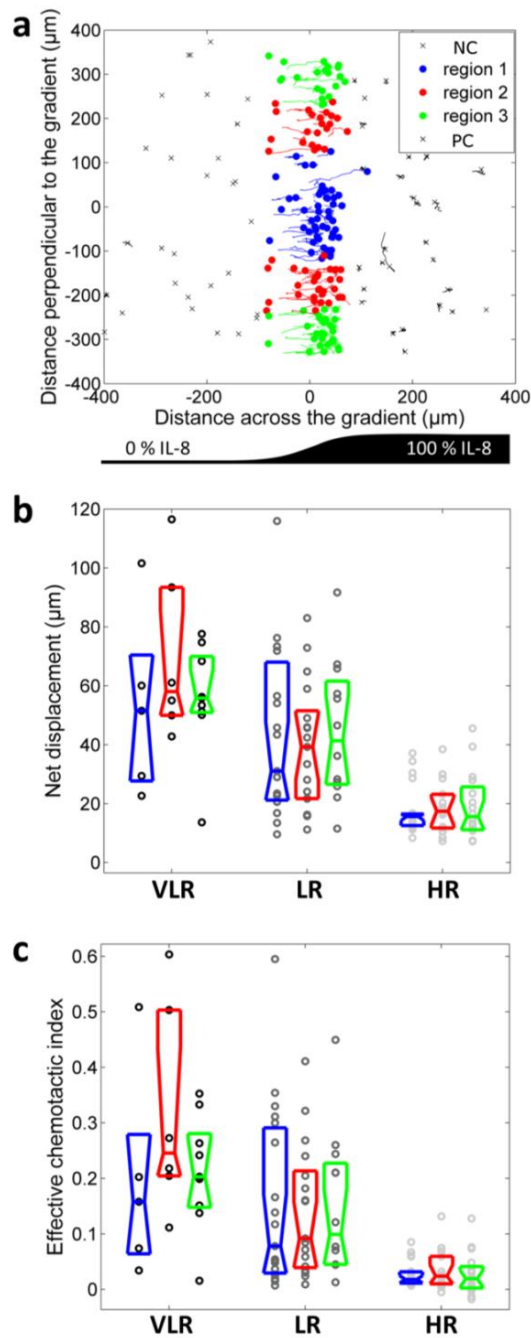


Figure S7. Neutrophil migration as a function of shear stress under stationary IL-8 concentration gradients. Flow induced shear stress did not significantly influence neutrophil migration. **(a)** Tracks of neutrophils in both control regions and in the gradient region. The gradient region is divided into three subregions with different ranges of applied shear stresses. **(b)** Net displacement of neutrophils in the different shear stress subregions for each gradient group. **(c)** E.C.I. of neutrophils in the different shear stress subregions for each gradient group. No significant differences were found between the three different shear stress groups within each gradient group.

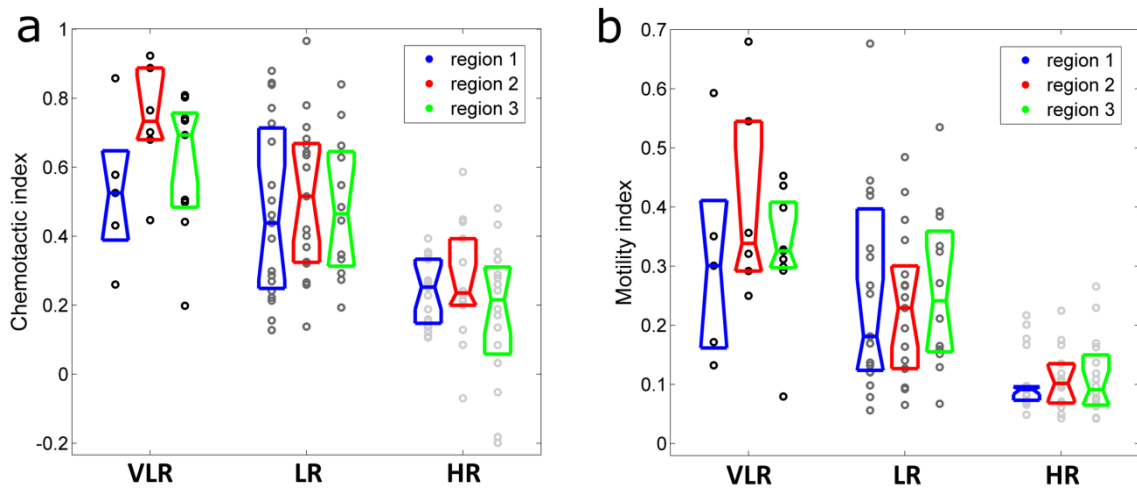


Figure S8. Effect of shear stress on neutrophil chemotaxis. Analysis of neutrophil migration under stationary IL-8 concentration gradients in three regions defined according to the Y distance from stagnation point. **(a)** Chemotactic index. **(b)** Motility index. Neutrophils that do not show any movement in experiments are eliminated from this analysis.

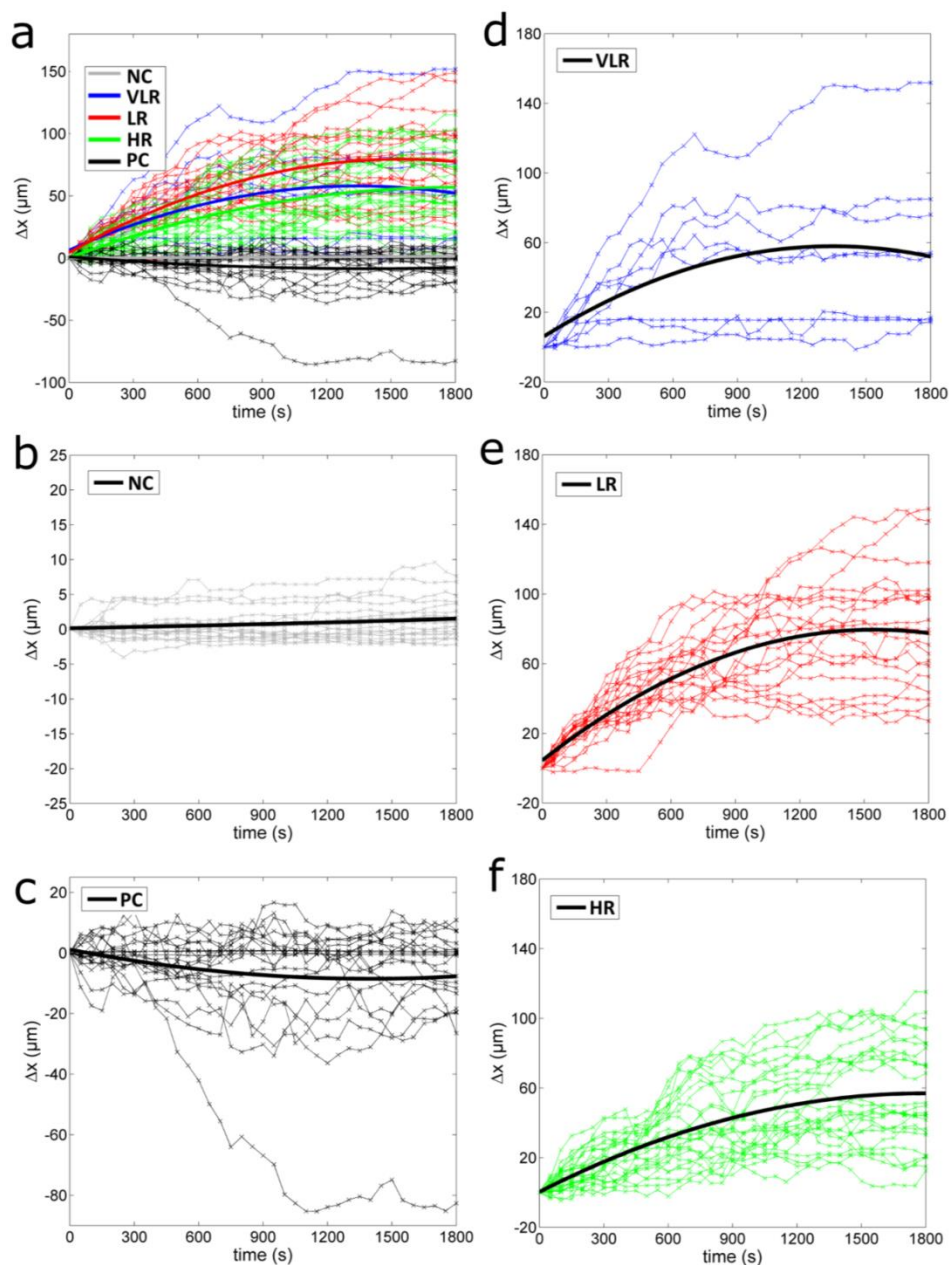


Figure S9. Analysis of individual neutrophils' migratory displacement under the moving gradient with respect to time. (a) Neutrophils in all groups. (b) Neutrophils in the NC group (negative control area). (c) Neutrophils in the PC group (positive area). (d) Neutrophils in the VLR group. (e) Neutrophils in the LR group. (f) Neutrophils in the HR group. Thick lines represent a second degree polynomial fitting the averaged data for each group.

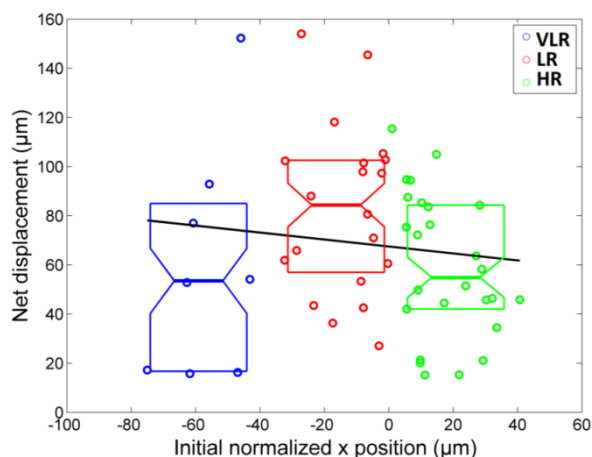


Figure S10. Neutrophils migration under a moving concentration gradient of IL-8. Net displacement of migrating neutrophils is weakly correlated ($R^2 = 0.012$) to their initial position within the position of the moving gradient at $t = 0$ s. Neutrophils from LR & HR under moving gradients migrated longer distances than their peers from the stationary gradients (Figure S5), with p -values < 0.01 when comparing the mean values of LR & HR in both cases.

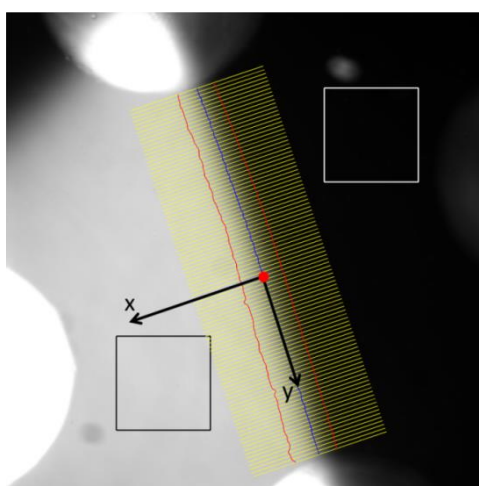


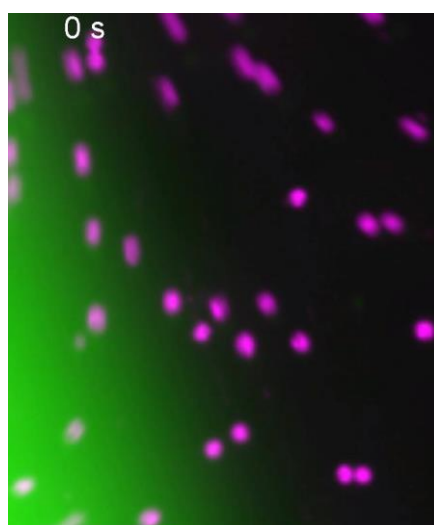
Figure S11. Analysis of the concentration gradients using a homemade MATLAB code. The software sums the time-lapse frames, and the user selects regions of 100% intensity (Black Square) and 0% gradient intensity (White Square). The user draws a line across the concentration gradient near each of the MFP's aspiration aperture, and the software approximates the 50% gradient intensity point along these lines and creates a segment joining both points as a first approximation of the 50% gradient intensity line. The software then creates one hundred intensity profiles (yellow) across the gradient, uniformly distributed along the y axis and centered on the approximated 50% gradient intensity line. Finally, the software finds the points of 10%, 50%, and 90% on each of the 100 intensity profiles and draws lines by connecting the points (red for the 10% and 90% intensity lines, and blue of the 50% intensity line).

Table S1. Definition of the neutrophils analysis parameters

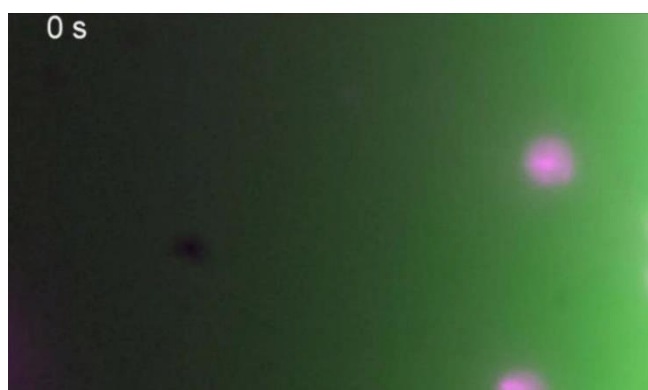
Parameter	Definition	Equation	Notes
Total distance (d)	Scalar quantity that refers to the length of the cell migration path.		Always positive
Net displacement (r)	Length of the vector quantity describing the overall change in position of the cell.		Always positive
Average cell speed (s)	Ratio of total distance (d) to the total time (Δt).	$s = \frac{d}{\Delta t}$	Always positive
Instantaneous speed	Speed of cell evaluated for a 50 s period.		Always positive
Average cell velocity (v)	Ratio of displacement of cells toward the gradient (Δx) to the total time (Δt).	$v = \frac{\Delta x}{\Delta t}$	Positive or negative
Instantaneous velocity	Velocity of cell evaluated for a 50 s period.		Positive or negative
Chemotactic index (C.I.)	Ratio of the displacement of cells toward the gradient (Δx) to the total migration distance (d).	$C.I. = \frac{\Delta x}{d}$	Positive or negative
Motility index (M.I.)	Ratio of displacement from starting position (r) to the maximum displacement (r_{max}).	$M.I. = \frac{r}{r_{max}}$ where $r_{max} = s_{max} \times \Delta t$	Always positive
Effective chemotactic index (E.C.I.)	Product of C.I. and M.I.	$E.C.I. = C.I. \times M.I.$	Positive or negative



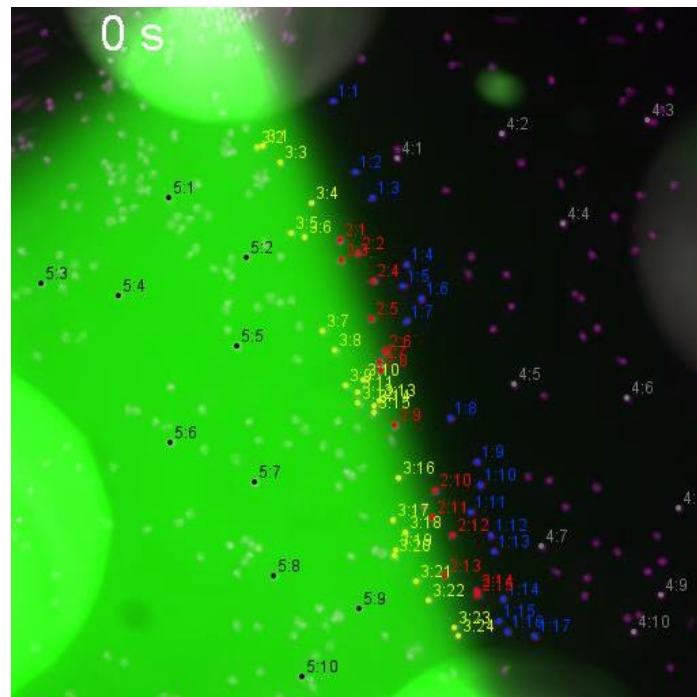
Video S1. Single neutrophil polarization and migration upon gradient exposure.



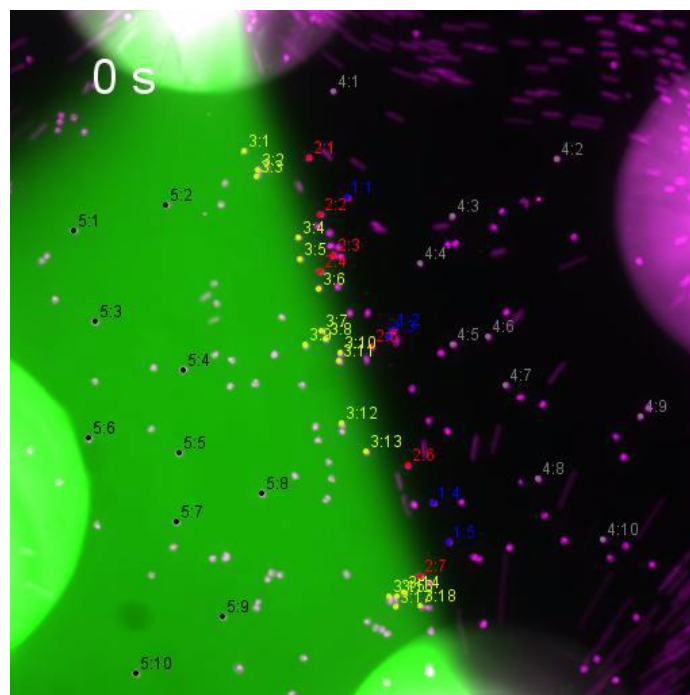
Video S2. Neutrophils rapid arrest upon entering the concentration gradient.



Video S3. Neutrophil rolling-like motion, adhesion, polarization, and migration.



Video S4. Tracks of individual neutrophils migrating within stationary gradient.



Video S5. Tracks of individual neutrophils migrating within moving gradient.